Journal of Advanced Research 29 (2021) 83–94

Contents lists available at ScienceDirect

Journal of Advanced Research

journal homepage: www.elsevier.com/locate/jare

Iminostilbene, a novel small-molecule modulator of PKM2, suppresses macrophage inflammation in myocardial ischemia–reperfusion injury

Shan Lu [a,b,c,d,e,1], Yu Tian [a,b,c,d,e,1], Yun Luo [a,b,c,d,e], Xudong Xu [a,b,c,d,e], Wenxiu Ge [f], Guibo Sun [a,b,c,d,e,*], Xiaobo Sun [a,b,c,d,e,*]

[a] Institute of Medicinal Plant Development, Peking Union Medical College and Chinese Academy of Medical Sciences, Beijing 100193, China
[b] Beijing Key Laboratory of Innovative Drug Discovery of Traditional Chinese Medicine (Natural Medicine) and Translational Medicine, China
[c] Key Laboratory of Bioactive Substances and Resource Utilization of Chinese Herbal Medicine, Ministry of Education, China
[d] Key Laboratory of efficacy evaluation of Chinese Medicine against glyeolipid metabolism disorder disease, State Administration of Traditional Chinese Medicine, China
[e] Key Laboratory of new drug discovery based on Classic Chinese medicine prescription, Chinese Academy of Medical Sciences, China
[f] College of Pharmacy, Harbin University of Commerce, Harbin 150076, Heilongjiang, China

GRAPHICAL ABSTRACT

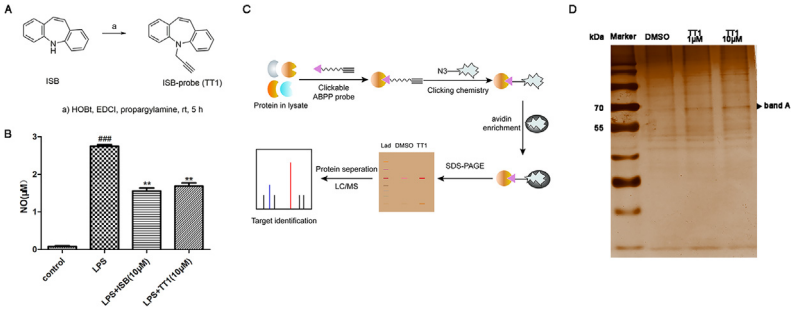

ARTICLE INFO

Article history:
Received 24 May 2020
Revised 29 August 2020
Accepted 2 September 2020
Available online 9 September 2020

Keywords:
Myocardial ischemia–reperfusion
Macrophage
Iminostilbene
Pyruvate kinase M2

ABSTRACT

Introduction: Inflammation is a key factor in myocardial ischemia/reperfusion (MI/R) injury. Targeting leucocyte-mediated inflammation is an important strategy for MI/R therapy. Iminostilbene (ISB), a simple dibenzoazepine small molecule compound, has a strong anti-neurodegenerative effect. However, no study has shown the cardioprotective effect of ISB.

Objectives: This study aimed to investigate the role of ISB against MI/R injury and identify its molecular target.

Methods: To verify the cardiac protection of ISB *in vivo* and *in vitro*, we performed rat MI/R surgery and subjected inflammatory modeling of macrophages. In terms of molecular mechanisms, we designed and synthesized a small molecular probe of ISB and employed it on the click chemistry-activity-based protein profiling technique to fish for ISB targets in macrophages. To identify the target, we applied the competitive inhibition assay, surface-plasmon resonance (SPR), cellular thermal shift assay (CETSA), and drug affinity responsive target stability (DARTS) assay.

Results: *In vivo*, ISB showed robust anti-myocardial injury activity by improving cardiac function, reducing myocardial infarction, and inhibiting macrophage-mediated inflammation. *In vitro*, ISB strongly inhibited the transcription and the expression levels of inflammatory cytokines in macrophages. The pyruvate

Peer review under responsibility of Cairo University.

* Corresponding authors at: Institute of Medicinal Plant Development, Chinese Academy of Medical Sciences & Peking Union Medical College, No. 151 Malianwa North Road, Haidian District, Beijing, China.
E-mail addresses: sunguibo@126.com (G. Sun), sun_xiaobo163@163.com (X. Sun).
[1] These authors contributed equally to this work.

https://doi.org/10.1016/j.jare.2020.09.001

kinase isozyme type M2 (PKM2) was identified as the potential target of ISB through proteomic analysis and the competitive assay was performed for specific binding verification. Further thermodynamic and kinetic experiments showed that ISB was bound to PKM2 in a dose-dependent manner. Moreover, in terms of the biological function of ISB on PKM2, ISB reduced the expression of PKM2, thereby reducing the expression of HIF1α and the phosphorylation of STAT3.

Conclusion: This study for the first time demonstrated that ISB targeted PKM2 to reduce macrophage inflammation thereby significantly alleviating MI/R injury.

Introduction

Myocardial infarction and its secondary reperfusion injury are the most common and clinically significant myocardial injury thereby resulting in increasing morbidity and mortality [1,2]. Myocardial ischemia/reperfusion (MI/R) injury involves many pathological factors, among which inflammatory response is an important feature [3]. Inflammation and inflammatory cell infiltration are indicators of MI/R injury [4,5]. Macrophages play a crucial role in the process of MI/R injury [6-8]. During the early phase of MI/R, proinflammatory monocytes/macrophages, which secrete a large number of inflammatory factors (such as interleukin-6 [IL-6] and interleukin-1β [IL-1β]), further aggravate the myocardial injury [9], rapidly infiltrate the injury site, and display a strong inflammatory phenotype [6,10,11]. The abundance of inflammatory macrophages is closely related to the adverse left ventricular remodeling[6]. Therefore, targeting inflammatory macrophage subtypes is an important anti-inflammatory strategy for improving MI/R injury.

Metabolic remodeling is closely related to the inflammatory state of macrophages. Inflammatory macrophage subtypes rely on glycolysis for ATP generation [12-14]. Some glycolytic kinases are involved in the inflammatory response of macrophages [12,15]. Pyruvate kinase isozyme type M2 (PKM2), a rate-limiting enzyme in the glycolytic pathway, functions as an important regulator of inflammation in LPS-stimulated macrophages [16]. As a transcriptional coactivator, PKM2 forms a complex with hypoxia-inducing factor alpha (HIF-1α) that enhances transcription of IL-1β by binding to its promotor in response to LPS [17-19]. In addition, PKM2 functions as a protein kinase and phosphorylates the transcription factor STAT3, thereby boosting IL-6 and IL-1β production [20,21]. Thus, targeting PKM2 to regulate the metabolic remodeling of macrophages may provide a new method for the treatment of inflammatory diseases.

For small organic molecules, nitrogen-containing heterocyclic alkaloid-type compounds have attracted much attention because of their extensive biological activities and important pharmacophore [22]. Dibenzoazepine derivatives, which are a class of important heterocyclic compounds, have a wide range of pharmacological effects including antidepressive, antiepileptic, analgesic, anticancer, antidiabetic, and anti-inflammatory activities [23–28]. Some synthetic dibenzoazepine derivatives have also been reported to possess cardioprotective activities. For example, a dibenzoazepine derivative, as a GPR4 antagonist, can effectively improve myocardial infarction in mice [29]. The research on the heart protection of dibenzoazepine derivatives has a broad prospect. Hajieva *et al.* have evaluated different aromatic amines and aromatic imines and found that iminostilbene (ISB) has strong antiapoptotic, antioxidant and neuronal protective properties *in vitro* and worked at low concentrations of sodium molarity [30,31]. ISB, as a simple dibenzoazepine small molecule compound, has a strong antineurodegenerative effect. However, no study has shown the cardioprotective effect of ISB, and the molecular mechanisms and potential targets remain to be elucidated.

The activity-based protein profiling (ABPP), a chemical proteomic technique, identifies the potential targets of compounds with small molecular probes [32–38]. With the development and progress of chemical biology, click chemistry (CC) strategy is introduced into the design of small-molecule probe to reflect the change in functional state of the target protein in cells [32]. In this study, we first investigated the role of ISB against MI/R injury and its underlying mechanism in macrophage inflammation, and subsequently identified its molecular target using the CC-ABPP technology. Additionally, we speculated that ISB alleviated MI/R injury by modulating macrophage inflammation via targeting PKM2.

Materials and methods

Experimental materials

ISB (≥98% purity) was purchased from Aladdin (Shanghai, China). DiltiazemHydrochloride Tablets (DTZ) was obtained from Tianbian Pharmaceutical Co., Ltd. (Tianjin, China). The primary antibody against COX2, IL-1β, HIF1α, STAT3 and p-STAT3 was obtained from Abcam (Cambridge, UK), and the primary antibody against Bax, Bcl2 and Caspase-3 was obtained from Proteintech (Wuhan, China). The PKM2 primary antibody was from CST (Boston, USA). The recombinant human PKM2 protein was from Abcam (Cambridge, UK). The rest of the reagents were from Sigma (Merck KgaA, Germany).

Animals

Male adult Sprague-Dawley rats (240–280 g) were purchased from Beijing Vital River Laboratory Animal Technology Co., Ltd. (Beijing, China). SD rats were housed for three days before experiments under standard laboratory conditions. The rats were randomly divided into five experimental groups, namely, sham, I/R, 0.625 mg/kg ISB, 1.25 mg/kg ISB and 16 mg/kg DTZ groups. ISB and DTZ were suspended in 0.5% (w/v) aqueous solution of carboxymethylcellulose and stored at 4 °C. ISB and DTZ table gavage were performed five days prior to the ischemic operation.

Compliance with ethic requirements

The use of animals was approved by the Laboratory Animal Ethics Committee of the Institute of Medicinal Plant Development, Peking Union Medical College, and conformed to the Guide for the Care and Use of Laboratory (approve number: SLXD-20190711001).

Myocardial ischemia/reperfusion model

The rats were anesthetized through the intraperitoneal injection of pentobarbital sodium (40 mg/kg), intubation in the supine position, and monitoring using electrocardiogram. The chest was then opened, and the left anterior descending (LAD) coronary artery was ligated over a tube with a thread from 2 mm below

the left atrial appendage [39]. Heart ischemia began when the ST segment of the ECG raised, and lasted for 30 min. Following ischemia, the hearts were reperfused for 24 h or 7 days. The sham group was subjected to the same procedures but without ligation.

Determination of infarct size

After all treatment, the heart was removed, rinsed with saline, and frozen using liquid nitrogen for 1 min. Along the heart axis, the heart was cut into six slices and incubated in 2% TTC (Sigma-Aldrich; Merck KgaA, Germany) for 15 min at 37 °C in the dark. After 4% paraformaldehyde was fixed for 24 h, the heart slices were collected and photographed for preservation. Image J was used to analyze the infarct (white) and non-infarct (red) areas. The percentage of myocardial infarct was calculated as the infarct area divided by total area.

Myocardial injury indicators of rat serum determination

The levels of creatine kinase MB isoenzyme (CK-MB), lactate dehydrogenase (LDH) in the serum at 24 h after reperfusion were detected using a biochemical analyzer. The troponin (cTnT) level was detected at 24 h after reperfusion using enzyme-linked immunosorbent assay (ELISA) kit (EXPANDBIO, Beijing, China) in accordance with the instructions.

Histopathological examination and immunohistochemical analyses

The heart tissue was fixed with 4% paraformaldehyde and embedded in paraffin. Subsequently, the heart tissue sections were heated, deparaffinised, and dehydrated before staining with haematoxylin and eosin (HE). Then the pathological changes of heart tissue were detected with Aperio S2 Leica Biosystem microscopy (Leica, Wetzlar, Germany). In addition, TUNEL was used to detect apoptosis in tissue sections in accordance with the reagent instructions.

The immunohistochemical staining was carried out using SP Rabbit&Mouse HPR kit (CoWinBiosciences, Beijing, China). Briefly, the sections were heated, deparaffinised, and dehydrated. Their antigen was repaired, and the endogenous peroxidase was blocked. The sections were then incubated in a suitable primary antibody solution at 4 ℃ overnight, followed by incubation with the corresponding secondary antibody solution. The slides were stained using the DAB kit, restained with hematoxylin, and observed using Aperio S2 Leica Biosystem microscopy (Leica, Wetzlar, Germany).

Echocardiography

Cardiac contractile function was evaluated through transthoracic M−mode echocardiography by using the Vevo 2100 system (VisualSonics).

Immunofluorescence staining

The frozen sections were incubated with 1% Triton for 15 min at room temperature following with Proteinase K working fluid for 30 min. Then the frozen sections were blocked with BSA at room temperature for 1 h and incubated with primary antibodies against iNOS (1:100, Abcam) or CD68 (1:100, Abcam) overnight at 4 °C. The next day, the sections were incubated with secondary antibody at 37 °C in the dark for 1 h. Then nuclei were stained with DAPI. The fluorescent images were acquired by Tissue Gnostics AX10 analysis system (Vienna, Austria).

Raw264.7 macrophage culture and drug treatment

Raw264.7 macrophage was obtained from the National Infrastructure of Cell Line Resource (Beijing, China), and cultured in DMEM containing 10% FBS, 100 U/mL penicillin, and 100 μg/mL streptomycin and was maintained at 37 °C in 5% CO2. ISB was dissolved in DMSO as stock solution and diluted with DMEM basic medium. The cells were seeded into various plates and pretreated with ISB for 6 h, and then stimulated with LPS (100 ng/mL) for corresponding time.

Nitric oxide (NO) content determination

Cytokine NO generally exists in the supernatant in the form of nitrate or nitrite. The Griess reaction method was used to determine the total nitrite concentration to reflect the release level of NO in cells. The operation was carried out in accordance with the instructions of the NO assay kit (Beyotime, Shanghai, China). Briefly, macrophages were incubated with ISB (i.e., 2.5, 5 and 10 μM) for 6 h and incubated with 100 ng/mL LPS for 24 h. The collected cell supernatant was added into the 96-well plate, followed by the Griess reagent. After the color was stabilized, the absorbance was measured at 540 nm by using a Synergy H1 microplate reader (BioTek, Vermont, USA).

RNA extraction and quantitative real-time PCR (qPCR) analysis

Total RNA was isolated from macrophage lysates and the rat hearts in the infarct zone using Trizol reagent (Invitrogen, USA). High-quality RNA was quantified by ultraviolet analysis. The isolated RNA was reverse transcribed to cDNA by using PrimeScript™ RT reagent Kit with gDNA Eraser (TaKaRa). cDNA was subjected to Real-time PCR using SYBR Premix Ex Taq™ (TaKaRa) with lightcycler® 480II (Roche). The primer pairs used in this study were listed in Table 1. GAPDH was used for normalization of mRNA expression. Fold change was calculated using the $2^{-\Delta\Delta CT}$ method.

Cytokine Enzyme-Linked immune sorbent assay (ELISA)

IL-6, IL-1β and MCP-1 levels were measured in the media collected from RAW264.7 at 6 h after stimulation with LPS (100 ng/mL), or in the serum of rats with MI/R by using a commercial ELISA kit (EXPANDBIO, Beijing, China) in accordance with the manufacturer's instructions.

Western Blots

Protein was isolated from macrophage lysates and the rat hearts in the infarct zone. Western blots were performed according to reported protocols [39]. Briefly, 40 μg of total proteins were loaded per lane, separated using 10% SDS-PAGE, and blotted onto nitrocellulose membranes. The membrane was incubated overnight with primary antibody. The membranes were washed and incubated with the corresponding secondary antibody. Finally, the bands were visualised using an ECL kit (CW0049, CWBIO, Beijing, China).

CC-ABPP assay

Macrophages were lysed in PBS buffer. The protein concentration was determined using the BCA protein assay and normalized to 5 mg/mL. Then, 0.4 mL cell homogenate were collected and incubated for 1 h with DMSO and TT1 (1 and 10 μM) of the same volume at room temperature. Then click reaction reagents were added and reacted for 1 h. The samples were incubated with streptavidin beads for 2 h. After sample underwent the centrifugation, the supernatant was absorbed, and then a 2 × loading buffer was

Table 1
Primers used for quantitative real-time PCR.

Gene	Primer sequence (5′ to 3′)	Species
GAPDH	F: CTGCGGCATCCACGAAACT R: AGGGCCGTGATCTCCTTCTG	mouse
IL-1β	F: TGCCACCTTTTGACAGTGATGA R: TGTGCTGCTGCGAGATTTGA	mouse
iNOS	F: CTGCAGCACTTGGATCAGGAACCTG R: GGAGTAGCCTGTGTGCACCTGGAA	mouse
COX2	F: CAGTTTATGTTGTCTGTCCAGAGTTTC R: CCAGCACTTCACCCATCAGTT	mouse
TNFα	F: AAACCACCAAGTGGAGGAGC R: ACAAGGTACAACCCATCGGC	mouse
IL-1β	F: CCCAACTGGTACATCAGCACCTCTC R: CCTGGGGAAGGCATTAGGAATAGTG	rat
IL-6	F: GATTGTATGAACAGCGATGATGC R: AGAAACGGAACTCCAGAAGACC	rat
GAPDH	F: TTCCTACCCCCAATGTATCCG R: CCACCCTGTTGCTGTAGCCATA	rat

added. The sample was mixed using a vortex and the protein was boiled for 5 min in a constant-temperature metal bath at 98 ℃ to denature the protein. The supernatant was centrifuged and retained for western blot analysis or sliver staining before processing for LC-MS/MS.

Cellular thermal shift assay (CETSA)

CETSA was performed in accordance with a previous study [40]. Briefly, the collected macrophages were lysed with kinase buffer and centrifuged at 12000 rpm for 20 min, and the supernatant was retained. The macrophage lysates were divided into two groups, namely, the DMSO and the 40 μM ISB groups. Each group was divided into eight equal parts and heat-treated at 46, 50, 54, 58, 62, 66, and 70 ℃ for 3 min. Then, the DMSO and 40 μM ISB groups were quickly transferred to ice and centrifuged at 12 000 rpm with a cryogenic centrifuge for 10 min. The supernatants were obtained, added with loading buffer, and analyzed using Western blot.

Drug affinity responsive target stability (DARTS) assay

DARTS assay was performed according to a previous study [41]. Briefly, the collected macrophages were lysed with NP40 lysate containing protease inhibitor and centrifuged at 12000 rpm for 20 min. The supernatant was retained and the TNC buffer was added. The experiment was divided into seven groups, and 100 μL cell lysate was collected from each group. One group was the control group, and the other six groups were the experimental groups. The lysates in the experimental groups were added with varying concentrations of ISB (0, 5, 10, 20, and 40 μM), allowed to stand at room temperature for 1 h, and added with pronase (25 $\mu g \cdot mL^{-1}$). After 30 min at room temperature, the reactions were stopped by adding the loading buffer and analyzed via Western blot.

Surface-plasmon resonance (SPR)

The Pioneer System was used for SPR analysis and detection. The recombinant human PKM2 protein was immobilized on the COOH5 Sensor Chip via 400 mM EDC/100 mM NHS-mediated crosslinking reaction. ISB and TT1 were dissolved in 100% DMSO to obtain a concentration of 5 mM and diluted in running buffer at concentrations ranging from 3.125 μM to 100 μM. The flow rate is 30 μL/min. The protein contact time was set to 60 s, and the dissociation time was set to 120 s. Data were analyzed using the Pioneer SPR System.

Statistical analysis

Data were collected and analysed blindly, and were presented as mean ± SD. Statistical analyses were performed using GraphPad Prism 5.0. One-way ANOVA followed by Tukey's post-hoc test was used for multiple comparisons. The statistical significance was set at $P < 0.05$.

Results

ISB alleviated cardiomyocyte injury

We first investigated the *in vivo* myocardial protective effect of ISB in rat MI/R model. TTC staining showed that the I/R group exhibited severe myocardial infarction compared with the sham group, and the application of DTZ (positive control) and ISB reduced the myocardial infarct size (Fig. 1A and B). HE staining revealed the pathological features of myocardial damage. The IR group manifested severe myocardial fibre necrosis, inflammatory cell infiltration, haemorrhageand architecture disruption in the infarct zone (Fig. 1C). DTZ and ISB pretreatment significantly reduced the degree of myocardium injury (Fig. 1C). In addition, the serum levels of cardiac enzymes were measured at 24 h after reperfusion. Analysis of CK-MB, LDH and cTnT levels in serum showed that I/R caused extensive myocardial damage, whereas DTZ and ISB inhibited these levels in a dose-dependent manner (Fig. 1D-1F). The effects of ISB on cardiac functions were assessed by echocardiography at 7 days after reperfusion. As shown by the M−mode echocardiograms (Fig. 1G), there was significantly lower ejection fraction (EF) and fractional shortening (FS) in the MI/R rats compared with sham group at 7 days after MI/R. However, these cardiac functional abnormalities were significantly ameliorated in 16 mg/kg DTZ and 1.25 mg/kg ISB-treated MI/R mice, indicating that DTZ and ISB has the ability to improve cardiac function after I/R (Fig. 1H-1I).

ISB alleviated cardiomyocyte apoptosis

Apoptosis, an important cause of myocardial cell loss, aggravates inflammatory cell infiltration and inflammatory response during myocardial I/R injury [42,43]. The antiapoptotic activity of ISB was determined by TUNEL staining. The I/R group had more TUNEL-positive cells in the infarct zone than the sham group. The ISB pretreatment significantly reduced the number of TUNEL-positive cells (Fig. 2A and 2B). In addition, the immunohistochemical results of caspase-3 showed that ISB can significantly inhibit the expression of caspase-3 in the infarct zone (Fig. 2C and 2D). Western blot showed that compared with the sham group, the expression of pro-apoptosis protein Bax was significantly increased, while the expression of anti-apoptosis protein Bcl2 was significantly decreased in I/R group, which was reversed after ISB pretreatment (Fig. 2E and 2F). These results established that ISB exerted an antiapoptotic effect in rats with myocardial I/R injury.

ISB suppressed the inflammatory response after MI/R

We detected the expression levels of inflammatory substances in myocardial tissue and serum to investigate the effect of ISB on inflammatory response after inflicting MI/R injury. As shown in Fig. 3A-3D, the ISB pretreatment dramatically suppressed RNA and protein levels of the proinflammatory cytokines IL-1β and IL-6 compared with the I/R group. In addition, the expression of the inflammatory proteins COX2, iNOS, pro-IL-1β and cleaved IL-1β were detected by Western blot. Results indicated that ISB signifi-

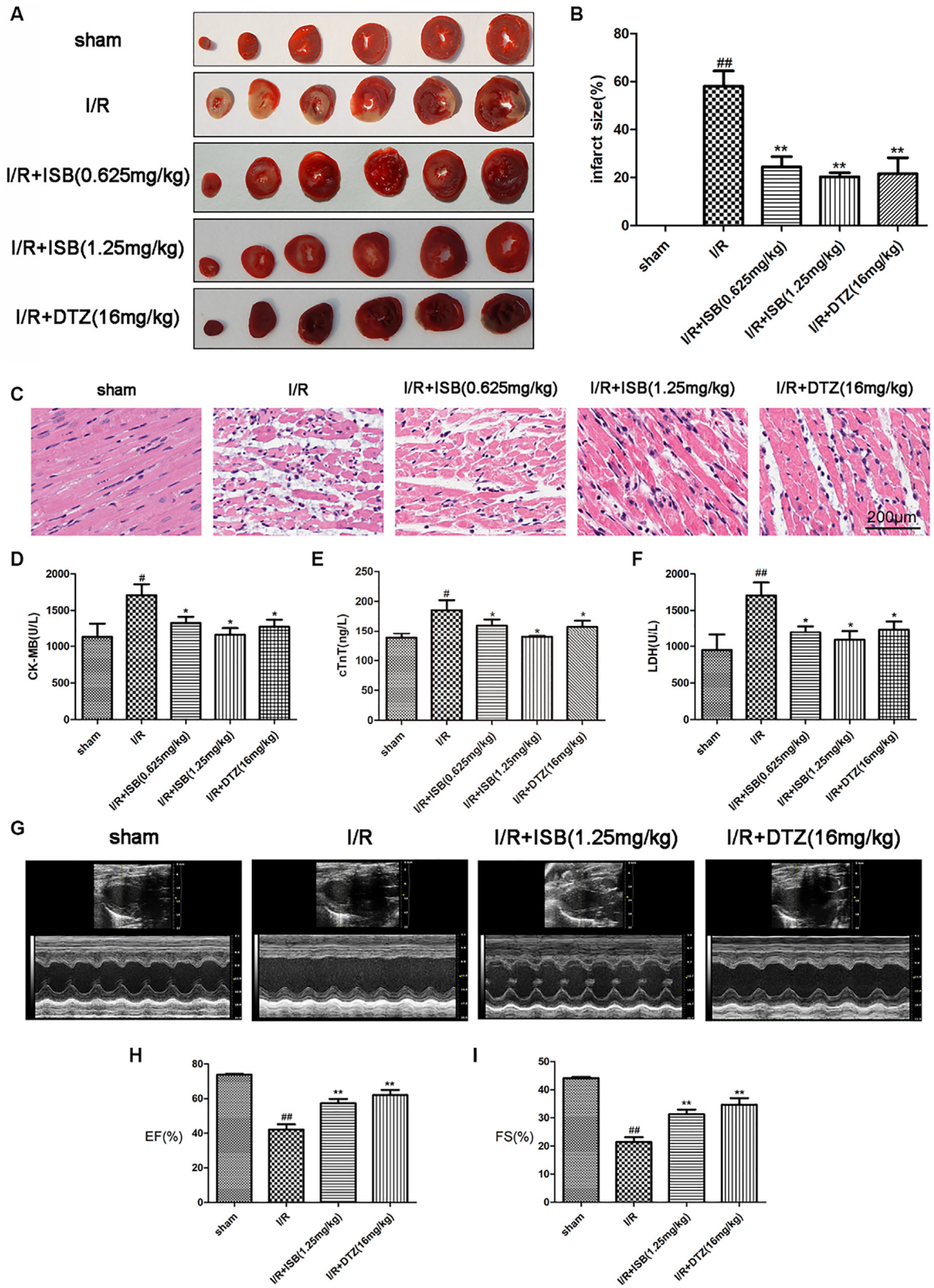

Fig. 1. ISB attenuated myocardial ischemia–reperfusion injury in rats. After ISB (0.625, 1.25 mg/kg) and DTZ (16 mg/kg) treatment for five days, the rats have undergone I/R surgery. (A) The representative images of TTC staining. (B) the TTC statistics graph was displayed. (C) The myocardial pathological damage was detected by HE staining. Scale bar, 200 μm. (D-F) The levels of CK-MB, cTnT and LDH were detected. (G) The representative echocardiographic graphs are presented. (H, I) The echocardiographic parameters were measured. Data are presented as means ± SD (n = 5). $^{\#}P < 0.05$, $^{\#\#}P < 0.01$ vs. the Sham group, $^{*}P < 0.05$, $^{**}P < 0.01$ vs. the I/R group.

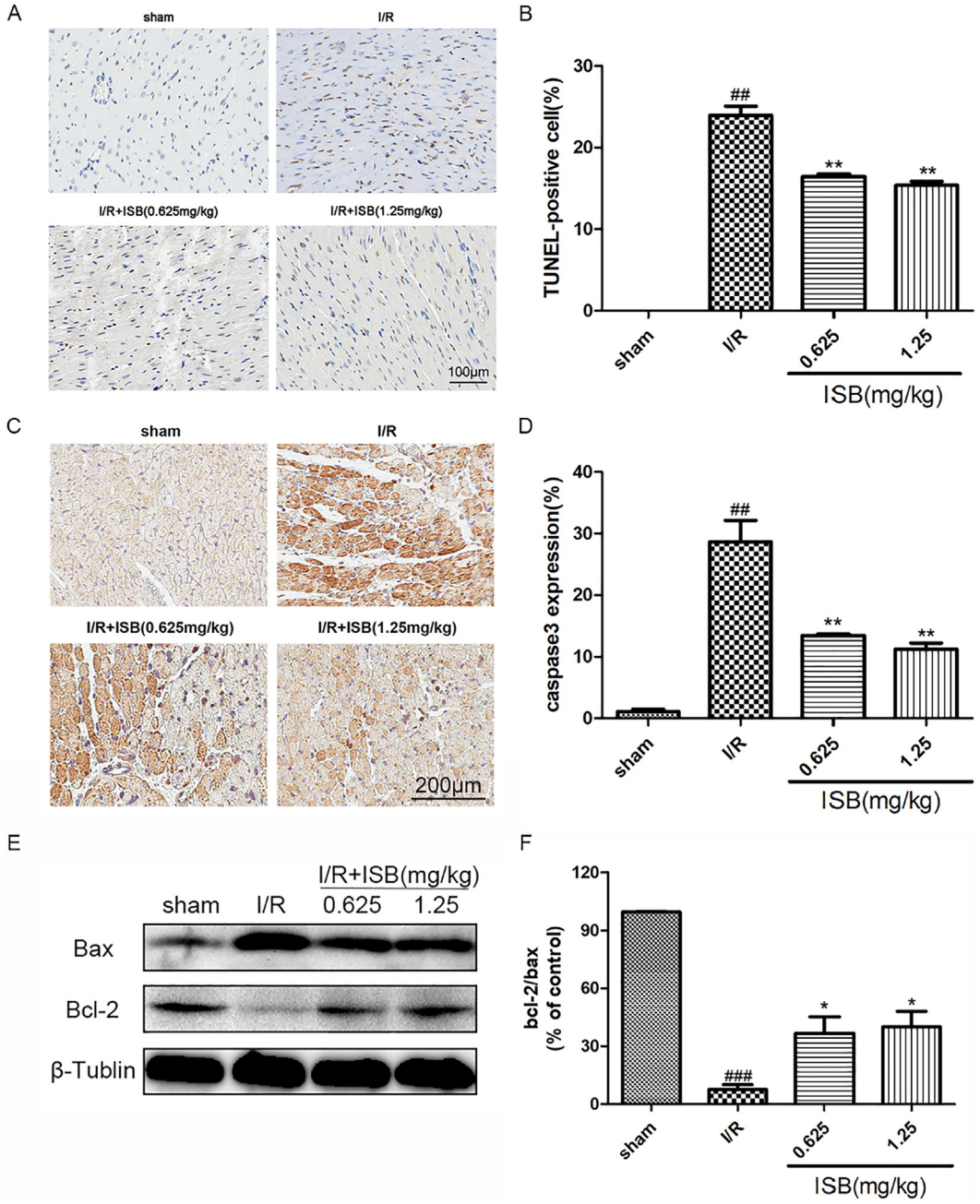

Fig. 2. ISB relieved myocardial apoptosis after MI/R in rats. (A) Representative images of TUNEL staining. Scale bar: 100 μm. (B) The analysis results of TUNEL-positive cells. (C-D) Immunohistochemical analysis of caspase-3 was displayed. (E) The representative western blot bands of Bax and Bcl2 in rat myocardial tissue. (F) Quantification of bcl-2/bax. The data were expressed as the mean ± SD (n = 3). $^{\#\#}P < 0.01$, $^{\#\#\#}P < 0.001$ vs. the Sham group, $^{*}P < 0.05$, $^{**}P < 0.01$ vs. the I/R group.

cantly decreased the expression of COX2 and iNOS and inhibited the activation of IL-1β (Fig. 3E and 3F).

ISB inhibited macrophage inflammation

Macrophages, which are important inflammatory effector cells, accumulate in the ischemic site after the occurrence of MI/R injury, participate in the formation of the microenvironment of myocardial inflammation, and affect the process of myocardial inflammatory response [3,44,45]. Therefore, the inhibition of inflammatory macrophages is important for the improvement of MI/R injury. To verify the relationship between the anti-inflammatory effect of ISB and macrophages, we used the surface markers of macrophages to identify the infiltration of macrophages after MI/R. The percentage of $CD86^{+}$ macrophages in the infarct zone was determined by immunohistochemistry. Analysis showed that $CD86^{+}$ macrophage infiltration increased in the I/R group. ISB treatment reduced the recruitment of proinflammatory macrophages after the occurrence of MI/R injury (Fig. 3G and 3H). Simultaneously, the immunofluorescence double staining results of iNOS and CD68 confirmed that the anti-inflammatory effect of ISB was related to the reduction of macrophage inflammation (Fig. 3I-K). Furthermore, we used LPS-induced macrophage inflammatory model to investigate the anti-inflammatory effect of ISB *in vitro*. First, we examined the effect of ISB on NO in RAW264.7 macrophages stimulated by LPS. As shown in Fig. 4A, ISB efficiently blocked LPS-induced NO release in a dose-dependent manner in RAW264.7 macrophages. Under LPS stimulation, macrophages pro-

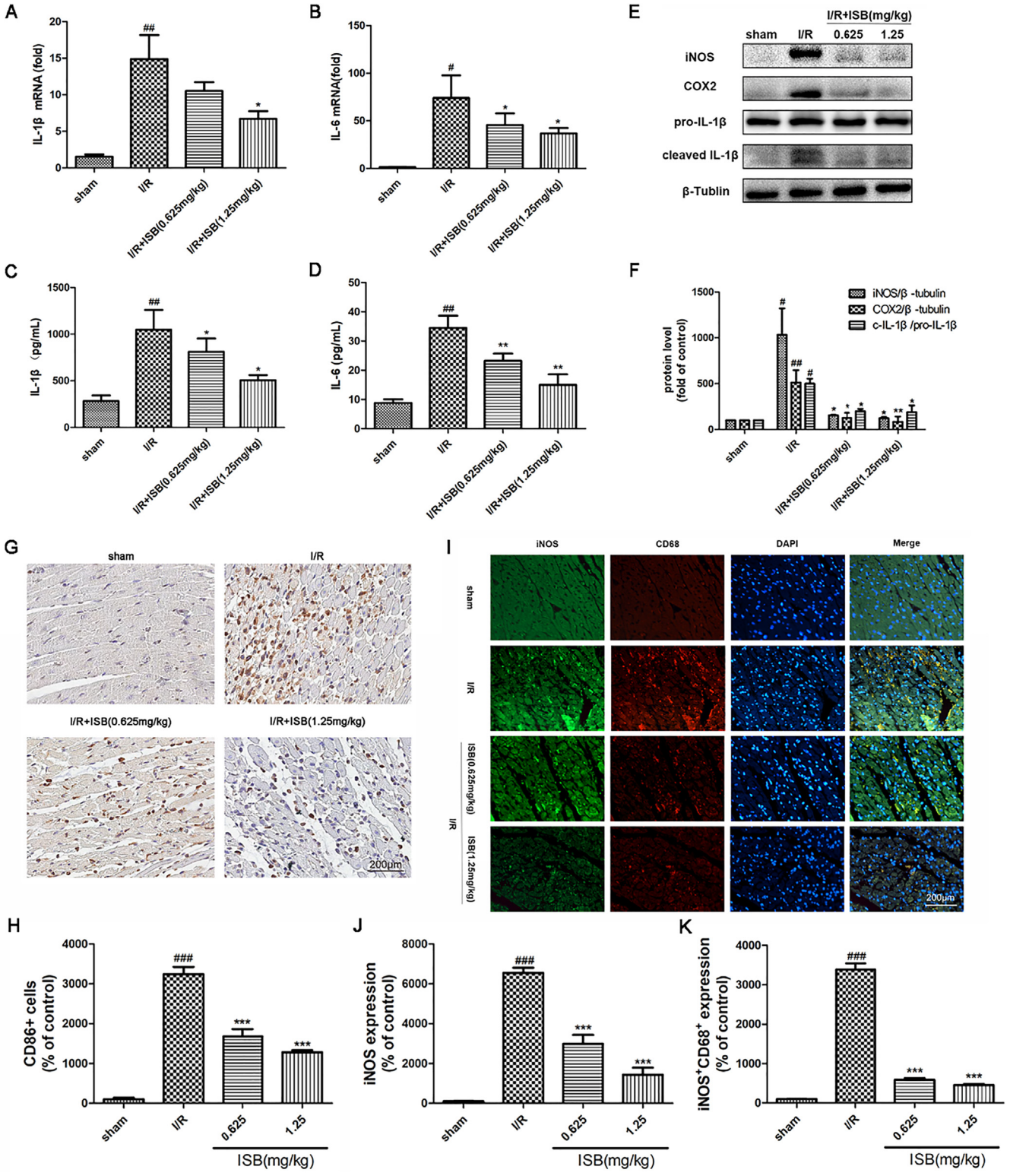

Fig. 3. ISB attenuated IR-induced inflammation in vivo. (A-B) mRNA levels of IL-1β and IL-6 in the hearts of rats quantified by real-time PCR. (C-D) The levels of IL- 1β and IL-6 in serum were measured by ELISA. (E) The representative western blot bands of iNOS, COX2, c-IL-1β, and pro-IL-1β in rat myocardial tissue. (F) The quantification of iNOS, COX2, c-IL-1β, and pro-IL-1β in rat myocardial tissue. (G) Immunohistochemical analysis of CD86 was displayed. (H) Statistical results of CD86-positive cells. (I) Dual immunofluorescence staining of iNOS (green) or CD68 (red) and DAPI (blue) in the hearts. (J) The fluorescence intensity of iNOS was statistically represented in the histogram. (K) Quantification of relative fluorescence intensity. The data were expressed as the mean ± SD (n = 3). $^{\#}P < 0.05$, $^{\#\#}P < 0.01$, $^{\#\#\#}P < 0.001$ vs. the Sham group, $^{*}P < 0.05$, $^{**}P < 0.01$, $^{***}P < 0.001$ vs. the I/R group.

duce many inflammatory factors, such as TNFα, IL-1β, IL-6, MCP-1, iNOS and COX2. Consistent with it, the enhanced concentrations of proinflammatory cytokines (i.e., IL-1β, IL-6, and MCP-1) in the LPS-stimulated RAW264.7 macrophage culture supernatant and the increased levels of inflammation-related genes (IL-1β, TNFα, iNOS and COX2) after LPS stimulation were markedly suppressed by

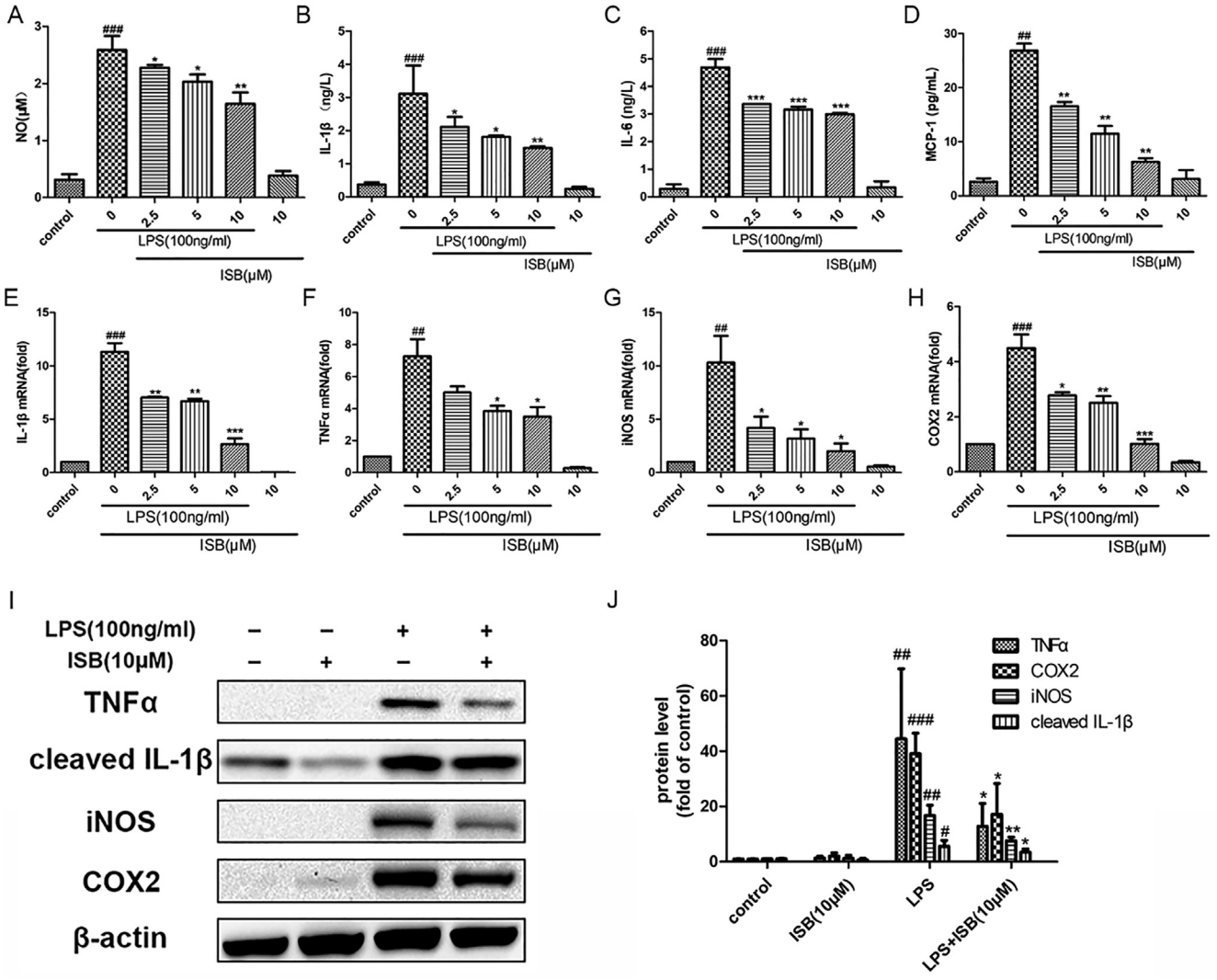

Fig. 4. ISB blocked LPS-induced macrophage inflammation *in vitro*. (A) NO levels in macrophages after stimulation with LPS ± ISB. (B-D) The levels of IL- 1β, IL-6 and MCP-1 in supernatants were measured by ELISA. (E-H) mRNA levels of macrophages IL-1β, TNFα, iNOS and COX2 quantified by real-time PCR. (I) The expression levels of TNFα, c-IL-1β, iNOS, COX2, and β-actin in the LPS-treated macrophages were displayed in western blots. (J) Statistical results of TNFα, c-IL-1β, iNOS and COX2 expression levels. The data were expressed as the mean ± SD (n = 3). $^{\#}P < 0.05$, $^{\#\#}P < 0.01$, $^{\#\#\#}P < 0.001$ vs. the Sham group, $^{*}P < 0.05$, $^{**}P < 0.01$, $^{***}P < 0.001$ vs. the I/R group.

treatment with ISB in a dose-dependent manner (Fig. 4B-H). In addition, the expression levels of COX2, iNOS, TNFα and cleaved IL-1β were assessed by Western blot analysis. 10 μM ISB preincubation before LPS stimulation significantly decreased the expression of COX2, iNOS, TNFα and cleaved IL-1β (Fig. 4I-4J). These results indicated that ISB inhibited macrophage inflammation.

Target identification

To identify the target of ISB, the ISB probe (TT1) was first constructed in this study. The probe synthesis process is shown in Fig. 5A. We examined the anti-inflammatory effects of ISB and TT1 to determine that the small molecule probe TT1 did not alter the biological activity compared to the original compound. We observed that TT1 showed similar inhibitory activity to ISB in LPS-stimulated macrophages, suggesting that TT1 can be used for the subsequent target fishing experiments (Fig. 5B). We used RAW264.7 macrophage to conduct target identification *via* CC-ABPP, as depicted in Fig. 5C. Briefly, TT1 and DMSO were fully interacted with macrophage protein lysates to proceed the click chemical reaction. Streptavidin beads were then used to capture proteins that interacted with ISB from the lysate. The proteome was eluted and separated by electrophoresis. As shown in Fig. 5D, the protein band at 55–70 kDa (band A) was most evident in the TT1 group, indicating that the protein in this band had a specific affinity to ISB and probably was the target protein of ISB. Therefore, the band was subsequently cut and subjected to enzymatic hydrolysis and LC-MS /MS identification. The identified peptide sequences were matched with the database. All the protein results were listed in Excel (Supplemental Data 2). During data processing, we used a strict cut-off fold change of 2 and score $\geq$ 5 as the qualification criterion [46]. Among the possible protein targets identified by proteomic analysis, PKM2 (58 kDa) had the highest protein matching score, and it has been shown to play a pivotal role in macrophage inflammation [17,47]. Therefore, we believed that PKM2 may be one of the potential targets of ISB against macrophage inflammation.

PKM2 as a potential target of ISB

We conducted a competitive inhibition experiment to evaluate the specific binding of ISB to PKM2. The protein that interacted

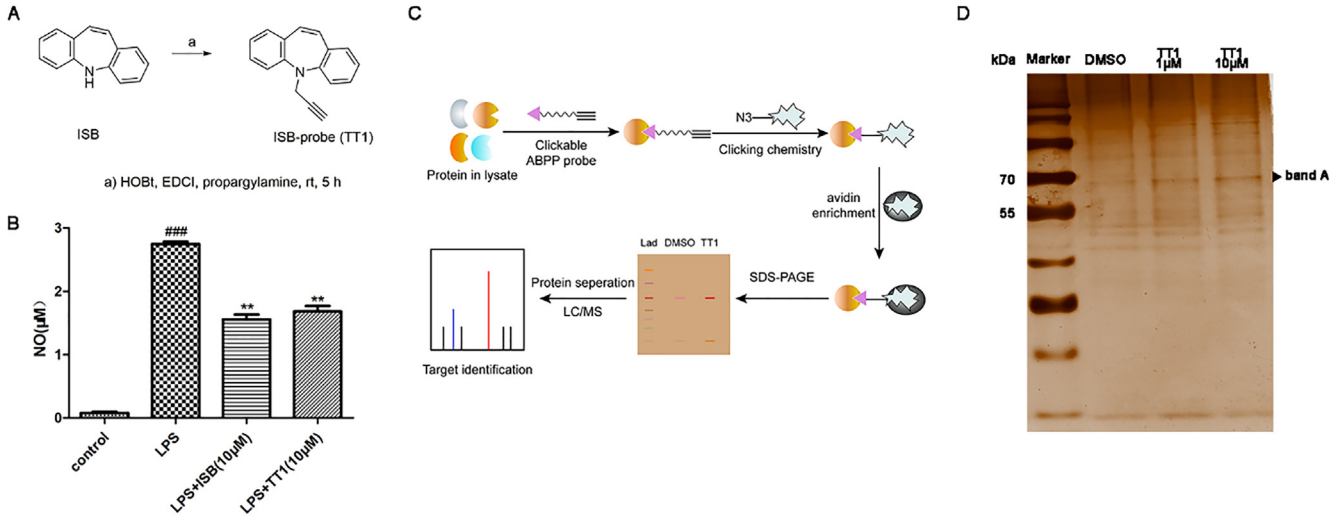

Fig. 5. Target identification of ISB. (A) Synthesis of biotinylated probe TT1. (B) TT1 inhibited the secretion of NO in LPS-induced macrophages. (C) Schematic diagram of target identification of TT1 in macrophages lysate. (D) Silver stained proteins co-precipitated with TT1. The data were expressed as the mean ± SD (n = 3). $^{###}P < 0.001$ vs. the Sham group, $^{**}P < 0.01$ vs. the I/R group.

with TT1 was captured from the lysate, and ISB was added to make it interact with the lysate. Given that TT1 and ISB had the same binding characteristics, ISB competed for the action site of protein and TT1, thereby reducing the amount of specific protein captured. Western blot analysis indicated that PKM2 was bound with TT1 efficiently, whereas excessive ISB reduces the binding of TT1 to PKM2 competitively. This result indicated that PKM2 had a specific affinity to ISB and was the target protein of ISB (Fig. 6A).

A series of target recognition methods were used to confirm the binding of ISB to PKM2 target protein. First, we used the cellular thermal shift assay (CETSA) to verify the target. When the target protein binds to small molecules, the configuration changes in the direction of low energy and high stability, and the ability to withstand high temperature increases. The protocols were similar to those reported previously [40]. As shown in Fig. 6B, in ISB-treated cell lysis solution, PKM2 has a stronger tolerance to high temperature, and the band strength of PKM2 was stronger than that of DMSO group at high temperature, indicating that PKM2 is the target of ISB. Simultaneously, we also used Drug Affinity Responsive Target Stability (DARTS) assay for verification. The principle of this experiment is that after the protein binds to small molecules, the protein structure changes in the direction of energy reduction and is more stable, and the resistance to protease increases [41,48]. Our data also demonstrated that after protease was added to the whole protein extract, the content of PKM2 decreased sharply, whereas ISB dose dependently increased the content of PKM2, indicating that ISB can improve the stability of PKM2 to protease (Fig. 6C).

Surface plasmon resonance (SPR) can track the interaction between biomolecules in the natural state in real time and evaluate the intermolecular binding force. SPR is also used to determine the interaction between ISB and PKM2. As shown in Fig. 6D and 6E, SPR data analysis revealed that both ISB and TT1 can bind to PKM2 in a dose-dependent manner. ISB interacted with recombinant PKM2 protein with a KD of 18.6 μM (Fig. 6D). TT1 interacted with recombinant PKM2 protein with a KD of 40.0 μM (Fig. 6E).

PKM2 is a regulatory protein with complex functions and plays a regulatory role in tumor and inflammatory diseases. Therefore, we examined the regulatory effect of ISB on PKM2. We first examined the effect of ISB on LPS-induced PKM2 expression in macrophages. Our results showed that 10 μM ISB pretreatment significantly inhibited the LPS induced PKM2 expression (Fig. 6F). In addition, PKM2 can exert biological functions through protein–protein interactions. It's documented that PKM2 formed a complex with HIF-1α, promoting the transactivation of HIF-1α target genes, such as IL-1β. PKM2 also phosphorylated the transcription factor STAT3, following boosting the production of IL-1β and IL-6, which shared binding sites for STAT3 [16,20]. To explore the effect of ISB on PKM2-interacting proteins, we examined the expression of HIFα and STAT3 proteins. As shown in Fig. 6G and 6H, treatment with 10 μM ISB downregulated the expression of HIF1α, accompanied by parallel decreases in the phosphorylation and expression of STAT3 in macrophages.

Discussion

The ischemia myocardium is improved by the reperfusion of coronary blood flow, but the reperfusion itself causes the myocardial death [4]. Many heart protection strategies have been tested on experimental animals over the past few decades, but clinical results have been disappointing. Moreover, no consensus on treatment is available [49]. Great effort is needed to seek novel therapeutic strategies to modulate MI/R injury. Here, we present evidenced that ISB may be a new potential agent for protection against MI/R injury. ISB significantly improved cardiac function, reduced myocardial apoptosis, and inhibited reperfusion induced inflammation. ISB dramatically reduced inflammatory cells especially inflammatory macrophage infiltration, thereby reducing macrophage inflammation. The inflammatory response inhibited by ISB is related to the metabolic remodeling of macrophages, and PKM2, which is the key enzyme of glycolysis, may be a potential target for ISB to regulate the inflammatory response.

There are many pathological changes in MI/R injury, among which inflammation and apoptosis are two central aspects. Inflammation and apoptosis are interdependent in the pathological process of MI/R. Myocardial ischemia and reperfusion can trigger apoptosis, leading to loss of cardiomyocytes, thereby reducing cardiac function [50]. Cell apoptosis releases large amounts of intracellular material into the surrounding tissue space, which aggravates inflammatory cell infiltration and inflammatory response during myocardial I/R injury [42,43]. Moreover, when the ischemic myocardium recovers blood flow, due to the production of oxygen free radicals, the damaged cardiomyocytes release endogenous risk signals to recruit inflammatory cells to nest,

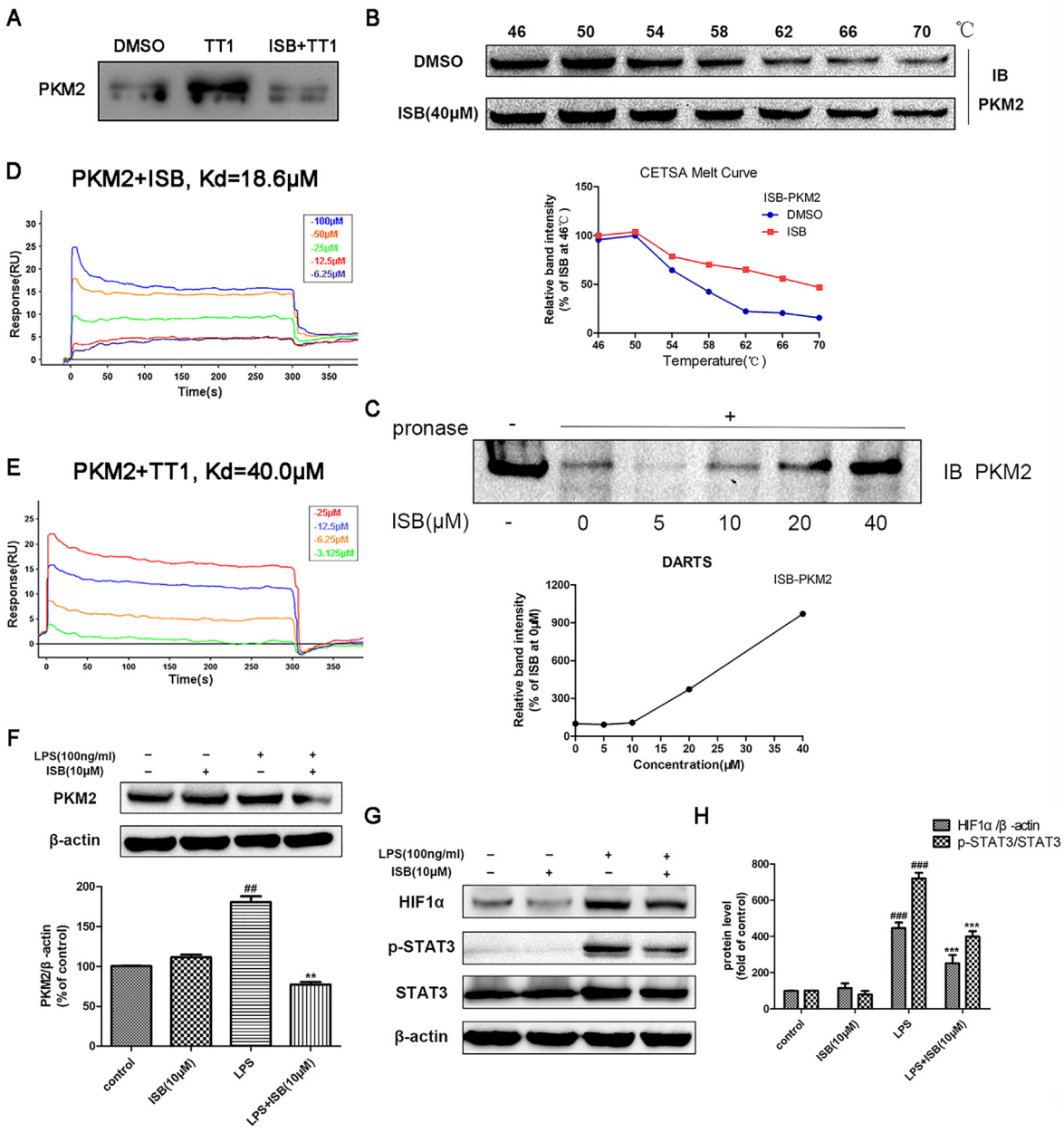

Fig. 6. PKM2 as potential target of ISB. (A) ISB competitively inhibited the binding of TT1 and PKM2. (B) CETSA assay is used to detect the effect of ISB on PKM2. (C) ISB promoted target protein PKM2 resistant to proteases (DARTS). (D-E) SPR analysed of ISB or TT1 binding to PKM2. (F) Effects of ISB on PKM2 expression levels in LPS induced macrophage inflammation. (G) HIF1α, STAT3 and p-STAT3 expressions were assayed by western blot analysis. (H) The quantification of HIF1α, STAT3 and p-STAT3 expression levels. Results were expressed as mean ± SD from at least three independent experiments. $^{\#\#}P < 0.01$, $^{\#\#\#}P < 0.001$ vs. the Sham group, $^{**}P < 0.01$, $^{***}P < 0.001$ vs. the I/R group.

start/amplify local inflammatory response, resulting in secondary damage of cardiomyocytes [51]. Inhibition of excessive inflammatory response can reduce the area of myocardial infarction and improve cardiac function [52,53]. It is confirmed that the local changes of I/R injury are mainly inflammatory reaction with neutrophil and monocyte infiltration [11,51]. Monocyte macrophages are the inflammatory cells with the longest resident time in myocardial injury and repair. Clinically, the increase of monocyte level is related to the aggravation of myocardial injury [54]. The anti-inflammatory strategy of targeting the inflammatory monocyte/macrophage subsets is a new research direction in improving myocardial reperfusion injury. In the present study, we have found that ISB reduced the release of inflammatory factors in a rat MI/R model. Subsequently, our results showed that the cardioprotection of ISB may be related to its inhibition of macrophage proinflammatory factor expression in myocardial tissue. *In vitro* experiments have also confirmed this view as ISB inhibited LPS-induced macrophage inflammation.

The target is the source and the biological material basis of drug action. Target identification is important for the development of new drugs and the elaboration of their pharmacological mechanisms. After confirming that ISB has good anti-inflammatory activity, the ISB probe was constructed as a tool for target identification. The anti-inflammatory target of ISB was fished from macrophages by using an ABPP-based chemical proteomic technology, and the anti-inflammatory mechanism of ISB was explored from the source. We have enriched the protein interaction with ISB from the total protein of macrophage by using molecular target fishing technology, and then determined that the target protein of ISB is PKM2 by LC-MS/MS. Then, we have determined the strong specific

binding of PKM2 to ISB through the competitive inhibition experiment. This result was validated again by using other target identification techniques, such as CETSA and DARTS assay. In addition, SPR results showed that ISB and PKM2 have moderate binding. Collectively, our study has confirmed that the target protein of ISB in macrophages is PKM2 and that the binding of PKM2 and ISB has strong specificity. However, more research is needed to prove the action model and the exact binding domain of ISB with PKM2.

The binding of ISB to PKM2 prompted us to investigate whether ISB inhibits LPS-induced PKM2 activation and prevents macrophage inflammation. Consistent with previous studies [16], our data suggested that LPS increases PKM2 expression, whereas ISB reverses this effect. Previous studies have established that PKM2 can stimulate HIF1α, which plays a key role in glycolysis and regulation of immune responses [17]. In addition, PKM2 contributes to the upregulation of STAT3 activation via the phosphorylation of STAT3 [55]. The inflammatory stimuli clearly cause the phosphorylation of STAT3, and the application of inhibitors of STAT3 reduces the expression levels of IL-1β and IL-6 in macrophages [20,56,57]. Our results indicated that in LPS-stimulated macrophages, ISB distinctly inhibited the expression of HIF1α, as well as the expression and phosphorylation of STAT3. However, the regulation of the binding of PKM2 to HIF1α and STAT3 by ISB and the specific binding sites of PKM2 should be further studied.

Conclusion

In summary, we confirmed for the first time that ISB can decrease myocardial infarction and apoptosis and inhibit inflammation, thereby reducing MI/R injury. These effects are related to the inflammatory inhibition in macrophages to a certain degree. In terms of mechanism research, we designed and synthesized the ISB probe for fishing out and verification of the target protein of ISB by the click reaction strategy and LC-MS/MS technology. Moreover, we have showed that PKM2 is a key target protein of ISB in macrophage and responsible for ISB's anti-inflammatory activity.

Declaration of Competing Interest

The authors declared that there is no conflict of interest.

Acknowledgments

This work was supported by Key Laboratory of new drug discovery based on Classic Chinese medicine prescription, Chinese Academy of Medical Sciences, China (Grant No. 2018PT35030), the Drug Innovation Major Project (Grant No. 2018ZX09711001-009), Peking Union Medical College Graduate Student Innovation Fund, China (Grant No. 2019-1007-16) and CAMS Innovation Fund for Medical Sciences(CIFMS) (Grant No. 2016-I2M-1-012).

Appendix A. Supplementary material

Supplementary data to this article can be found online at https://doi.org/10.1016/j.jare.2020.09.001.

References

[1] Ibáñez B, Heusch G, Ovize M, Van de Werf F. Evolving therapies for myocardial ischemia/reperfusion injury. J Am Coll Cardiol 2015;65:1454–71.
[2] Grant WR. Jeff rey ER, Christopher PC. Acute myocardial infarction. Lancet 2017;389:197–210.
[3] Timmers L, Pasterkamp G, de Hoog VC, Arslan F, Appelman Y, de Kleijn DPV. The innate immune response in reperfused myocardium. Cardiovasc Res 2012; 94: 276-283.
[4] Coert JZ, Antonio A, Hector AC, Michael VC, Massimo C, Dominique PV, et al. Innate immunity as a target for acute cardioprotection. Cardiovasc Res 2019;115:1131–42.
[5] Hofmann U, Frantz S. Role of lymphocytes in myocardial injury, healing, and remodeling after myocardial infarction. Cardiovasc Res 2015;116:354–67.
[6] Bajpai G, Schneider C, Wong N, Bredemeyer A, Hulsmans M, Nahrendorf M, et al. The human heart contains distinct macrophage subsets with divergent origins and functions. Nat Med 2018;24:1234–45.
[7] Hou X, Chen G, Bracamonte-Baran W, Choi HS, Diny NL, Sung J, et al. The cardiac microenvironment instructs divergent monocyte fates and functions in myocarditis. Cell Rep 2019;28:172–89.
[8] Heidt T, Courties G, Dutta P, Sager HB, Sebas M, Iwamoto Y, et al. Differential contribution of monocytes to heart macrophages in steady-state and after myocardial infarction. Circ Res 2014;115:284–95.
[9] Liu M, Yin L, Li W, Hu J, Wang H, Ye B, et al. C1q/TNF-related protein-9 promotes macrophage polarization and improves cardiac dysfunction after myocardial infarction. J Cell Physiol 2019;234:18731–47.
[10] Jia D, Jiang H, Weng X, Wu J, Bai P, Yang W, et al. Interleukin-35 promotes macrophage survival and improves wound healing after myocardial infarction in mice. Circ Res 2019;124:1323–36.
[11] Cao Y, Xu Y, Auchoybur ML, Chen W, He S, Qin W, et al. Regulatory role of IKKα in myocardial ischemia/reperfusion injury by the determination of M1 versus M2 polarization of macrophages. J Mol Cell Cardiol 2018;123:1–12.
[12] Nonnenmacher Y, Hiller K. Biochemistry of proinflammatory macrophage activation. Cell Mol Life Sci 2018;75:2093–109.
[13] Meiser J, Krämer L, Sapcariu SC, Battello N, Ghelfi J, D'Herouel AF, et al. Pro-inflammatory Macrophages Sustain Pyruvate Oxidation through Pyruvate Dehydrogenase for the Synthesis of Itaconate and to Enable Cytokine Expression. J Biol Chem 2016;291:3932–46.
[14] EL Kasmi KC, Stenmark KR. Contribution of metabolic reprogramming to macrophage plasticity and function. Semin Immunol 2015; 27: 267-275.
[15] De Souza DP, Achuthan A, Lee MKS, Binger KJ, Lee M, Davidson S, et al. Autocrine IFN-I inhibits isocitrate dehydrogenase in the TCA cycle of LPS-stimulated macrophages. J Clin Invest 2019;129:4239–44.
[16] Alves-Filho JC, Pålsson-McDermott EM. Pyruvate Kinase M2: A Potential Target for Regulating Inflammation. Front Immuno 2016;7:145.
[17] Palsson-McDermott EM, Curtis AM, Goel G, Lauterbach MAR, Sheedy FJ, Gleeson LE, et al. Pyruvate Kinase M2 Regulates Hif-1α Activity and IL-1β Induction and Is a Critical Determinant of the Warburg Effect in LPS-Activated Macrophages. Cell Metab 2015;21:65–80.
[18] Wang HJ, Hsieh YJ, Cheng WC, Lin CP, Lin YS, Yang SF, et al. JMJD5 regulates PKM2 nuclear translocation and reprograms HIF-1 -mediated glucose metabolism. P Natl Acad Sci 2014;111:279–84.
[19] Cheng Y, Feng Y, Xia Z, Li X, Rong J. ω-Alkynyl arachidonic acid promotes anti-inflammatory macrophage M2 polarization against acute myocardial infarction via regulating the cross-talk between PKM2, HIF-1α and iNOS. BBA-Mol Cell Biol L 2017;1862:1595–605.
[20] Yang P, Li Z, Li H, Lu Y, Wu H, Li Z. Pyruvate kinase M2 accelerates pro-inflammatory cytokine secretion and cell proliferation induced by lipopolysaccharide in colorectal cancer. Cell Signal 2015; 27: 1525-1532.
[21] Yang W, Lu Z. Regulation and function of pyruvate kinase M2 in cancer. Cancer Lett 2013;339:153–8.
[22] Al-Qawasmeh RA, Lee Y, Cao M, Gu X, Viau S, Lightfoot J, et al. 11-Phenyl-[b, e]-dibenzazepine compounds: Novel antitumor agents. Bioorg Med Chem Lett 2009;19:104–7.
[23] Mathieu O, Picot MC, Gelisse P, Breton H, Demoly P, Hillaire-Buys D. Effects of carbamazepine and metabolites on IL-2, IL-5, IL-6, IL-10 and IFN-gamma secretion in epileptic patients: the influence of co-medication. Pharmacol Rep 2011;63:86–94.
[24] Gómez CD, Buijs RM, Sitges M. The anti-seizure drugs vinpocetine and carbamazepine, but not valproic acid, reduce inflammatory IL-1β and TNF-α expression in rat hippocampus. J Neurochem 2014;130:770–9.
[25] Tomić M, Pecikoza U, Micov A, Vučković S, Stepanović-Petrović R. Antiepileptic drugs as analgesics/adjuvants in inflammatory pain: current preclinical evidence. Pharmacol Therapeut 2018;192:42–64.
[26] Sandra CM, Eduardo CC, Simon HO, Teresa RA, Antonio NC, Lijanova IV, et al. Anticancer activity and anti-inflammatory studies of 5-aryl-1,4-benzodiazepine derivatives. Anticancer Agents Med Chem 2012;12:611–8.
[27] Lee JTC, Shanina I, Chu YN, Horwitz MS, Johnson JD. Carbamazepine, a beta-cell protecting drug, reduces type 1 diabetes incidence in NOD mice. Sci Rep 2018;8:4588.
[28] Lin C, Lo S, Perng D, Wu DB, Lee P, Chang Y, et al. Complete Activation of Autophagic Process Attenuates Liver Injury and Improves Survival in Septic Mice. Shock 2014;41:241–9.
[29] Fukuda H, Ito S, Watari K, Mogi C, Arisawa M, Okajima F, et al. Identification of a Potent and Selective GPR4 Antagonist as a Drug Lead for the Treatment of Myocardial Infarction. ACS Med Chem Lett 2016;7:493–7.
[30] Moosmann B, Skutella T, Beyer K, Behl C. Protective activity of aromatic amines and imines against oxidative nerve cell death. Biol Chem 2001;382:1601.
[31] Hajieva P, Mocko JB, Moosmann B, Behl C. Novel imine antioxidants at low nanomolar concentrations protect dopaminergic cells from oxidative neurotoxicity. J Neurochem 2009;110:118–32.
[32] Wang S, Tian Y, Wang M, Wang M, Sun G, Sun X. Advanced activity-based protein profiling application strategies for drug development. Front Pharmacol 2018;9:353.

[33] Cravatt BF, Wright AT, Kozarich JW. Activity-based protein profiling: from enzyme chemistry to proteomic chemistry. Annu Rev Biochem 2008;77:383–414.
[34] Lee S, Nam Y, Koo JY, Lim D, Park J, Ock J, et al. A small molecule binding HMGB1 and HMGB2 inhibits microglia-mediated neuroinflammation. Nat Chem Biol 2014;10:1055–60.
[35] Liu Y, Fredrickson JK, Sadler NC, Nandhikonda P, Smith RD, Wright AT. Advancing understanding of microbial bioenergy conversion processes by activity-based protein profiling. Biotechnol Biofuels 2015;8:156.
[36] Wright MH, Sieber SA. Chemical proteomics approaches for identifying the cellular targets of natural products. Nat Prod Rep 2016;33:681.
[37] Parker CG, Kuttruff CA, Galmozzi A, Jørgensen L, Yeh C, Hermanson DJ, et al. Chemical proteomics identifies SLC25A20 as a functional target of the ingenol class of actinic keratosis drugs. ACS Central Sci 2017;3:1276–85.
[38] Dai J, Liang K, Zhao S, Jia W, Liu Y, Wu H, et al. Chemoproteomics reveals baicalin activates hepatic CPT1 to ameliorate diet-induced obesity and hepatic steatosis. P Natl Acad Sci 2018;115:E5896–905.
[39] Xu LJ, Chen RC, Ma XY, Zhu Y, Sun GB, Sun XB. Scutellarin protects against myocardial ischemia-reperfusion injury by suppressing NLRP3 inflammasome activation. Phytomedicine 2020;68:153169.
[40] Jafari R, Almqvist H, Axelsson H, Ignatushchenko M, Lundbäck T, Nordlund P, et al. The cellular thermal shift assay for evaluating drug target interactions in cells. Nat Protoc 2014;9:2100–22.
[41] Melody YP, Brett L, Heejun H, Robert S, William M, Joseph AL, et al. Drug affinity responsive target stability (DARTS) for small molecule target identification. Methods Mol Biol 2015;1263:287–98.
[42] Soares ROS, Losada DM, Jordani MC, Évora P, Castro-e-Silva O. Ischemia/reperfusion injury revisited: an overview of the latest pharmacological strategies. Int J Mol Sci 2019;20:5034.
[43] Toldo S, Mauro AG, Cutter Z, Abbate A. Inflammasome, pyroptosis, and cytokines in myocardial ischemia-reperfusion injury. Am J Physiol Heart Circ Physiol 2018;315:H1553–68.
[44] Rassaf T, Weber C, Bernhagen J. Macrophage migration inhibitory factor in myocardial ischaemia/reperfusion injury. Cardiovasc Res 2014;102:321–8.
[45] Bonaventura A, Montecucco F, Dallegri F. Cellular recruitment in myocardial ischaemia/reperfusion injury. Eur J Clin Invest 2016;46:590–601.
[46] Wei C, Zhao C, Liu S, Zhao J, Ye Z, Wang H, et al. Activity-based protein profiling reveals that secondary-carbon-centered radicals of synthetic 1,2,4-trioxolanes are predominately responsible for modification of protein targets in malaria parasites. Chem Commun 2019;55:9535–8.
[47] Yang L, Xie M, Yang M, Yu Y, Zhu S, Hou W, et al. PKM2 regulates the Warburg effect and promotes HMGB1 release in sepsis. Nat Commun 2014;5:4436.
[48] Park Y, Sun W, Salas A, Antia A, Carvajal C, Wang A, et al. Identification of multiple cryptococcal fungicidal drug targets by combined gene dosing and drug affinity responsive target stability screening. mBio 2016;7:e1016–73.
[49] Hausenloy DJ, Yellon DM. Ischaemic conditioning and reperfusion injury. Nat Rev Cardiol 2016;13:193–209.
[50] Gottlieb RA, Engler RL. Apoptosis in myocardial ischemia-reperfusion. Ann N Y Acad Sci 1999;874:412–26.
[51] Andreadou I, Cabrera-Fuentes HA, Devaux Y, Frangogiannis NG, Frantz S, Guzik T, et al. Immune cells as targets for cardioprotection: new players and novel therapeutic opportunities. Cardiovasc Res 2019;115:1117–30.
[52] Masaki F, Tetsuya M, Jun-ichiro K, Arihide O, Daiki F, Kaku N, et al. Nanoparticle incorporating Toll-like receptor 4 inhibitor attenuates myocardial ischaemia-reperfusion injury by inhibiting monocyte mediated inflammation in mice. Cardiovasc Res 2019;115:1244–55.
[53] Reiling J, Bridle KR, Schaap FG, Jaskowski L, Santrampurwala N, Britton LJ, et al. The role of macrophages in the development of biliary injury in a lipopolysaccharide-aggravated hepatic ischaemia-reperfusion model. BBA-Mol Basis Dis 2018;1864:1284–92.
[54] van der Laan AM, Hirsch A, Robbers LFHJ, Nijveldt R, Lommerse I, Delewi R, et al. A proinflammatory monocyte response is associated with myocardial injury and impaired functional outcome in patients with ST-segment elevation myocardial infarction. Am Heart J 2012;163:57–65.
[55] Samavati L, Rastogi R, Du W, Hüttemann M, Fite A, Franchi L. STAT3 tyrosine phosphorylation is critical for interleukin 1 beta and interleukin-6 production in response to lipopolysaccharide and live bacteria. Mol Immunol 2009;46:1867–77.
[56] Yang P, Li Z, Fu R, Wu H, Li Z. Pyruvate kinase M2 facilitates colon cancer cell migration via the modulation of STAT3 signalling. Cell Signal 2014;26:1853–62.
[57] Shirai T, Nazarewicz RR, Wallis BB, Yanes RE, Watanabe R, Hilhorst M, et al. The glycolytic enzyme PKM2 bridges metabolic and inflammatory dysfunction in coronary artery disease. J Exp Med 2016;213:337–54.